The MISR Calibration Program

CAROL J. BRUEGGE, DAVID J. DINER, AND VALERIE G. DUVAL

Jet Propulsion Laboratory, California Institute of Technology, Pasadena, California

(Manuscript received 6 September 1994, in final form 18 June 1995)

ABSTRACT

The Multiangle Imaging SpectroRadiometer (MISR) is currently under development for NASA's Earth Observing System. The instrument consists of nine pushbroom cameras, each with four spectral bands in the visible and near-infrared. The cameras point in different view directions to provide measurements from nadir to highly oblique view angles in the along-track plane. Multiple view-angle observations provide a unique resource for studies of clouds, aerosols, and the surface. MISR is built to challenging radiometric and geometric performance specifications. Radiometric accuracy, for example, must be within $\pm3\%/1\sigma$, and polarization insensitivity must be better than $\pm1\%$. An onboard calibrator (OBC) provides monthly updates to the instrument gain coefficients. Spectralon diffuse panels are used within the OBC to provide a uniform target for the cameras to view. The absolute radiometric scale is established both preflight and in orbit through the use of detector standards. During the mission, ground data processing to accomplish radiometric calibration, geometric rectification and registration of the nine view-angle imagery, and geophysical retrievals will proceed in an automated fashion. A global dataset is produced every 9 days. This paper details the preflight characterization of the MISR instrument, the design of the OBC, and the radiance product processing.

1. Introduction

MISR will acquire systematic multiangle imagery to monitor top-of-atmosphere and surface reflectances on a global basis, and to characterize the shortwave radiative properties of aerosols, clouds, and surface scenes. Data from the MISR experiment will enable advances in a number of areas concerning global change:

● *Clouds.* High-resolution bidirectional reflectances will be used in cloud classification, and the spatial and temporal variability of cloud hemispheric reflectance will be determined. Stereoscopic measurements will be used to retrieve cloud-top elevations. These data will help discern the role of different clouds types in the earth's energy balance.

● *Aerosols.* Multiangle radiance data will be used to determine aerosol optical depth and to identify particle composition and size distribution. These data will enable a global study of the role of aerosols on the energy budget and will provide data used for atmospheric correction of surface imagery.

● *Land surface.* Atmospherically corrected surface bidirectional reflectances will be used to estimate surface hemispheric reflectance, an important climate variable, and to characterize vegetation canopy structures.

These data will be important for investigating the effect of land surface processes on climate.

● *Oceans.* MISR will provide data to support ocean biological productivity studies in regions of low phytoplankton pigment concentrations, such as much of the tropical oceans.

2. Instrument

The MISR instrument, to be launched in 1998 as one of five instruments on the first Earth Observing System platform (EOS AM), will fly in a 705-km (440 mile) sun-synchronous descending polar orbit, with an equatorial crossing time of 1030 LT. The instrument will be used to produce registered global datasets from nine cameras and four spectral bands. The wavelength bands are nominally centered at 443, 555, 670, and 865 nm, with bandwidths varying between 15 and 25 nm. Data will be acquired with cross-track spatial sampling ranging from 275 m (250 m in the nadir) to 1.1 km (1.0 km in the nadir), depending on the "camera configuration," or onboard pixel averaging mode.

The terms "sampling," "pixel," and "instantaneous field-of-view" are commonly used within the remote sensing community. Sampling refers to the distance moved along the target between consecutive observations. The cross-track sampling distance is determined from the detector element width; downtrack sampling is controlled by an electronic shutter and the spacecraft velocity. At each sample position energy is collected by a detector element, producing an output digital number (DN) referred to as a pixel (a shorthand

for picture element). The physical target size that a detector element responds to is termed the instrument instantaneous field of view (IFOV). The downtrack IFOV is determined by the individual CCD detector dimensions and integration time, the target view angle, optical aberrations, and diffraction, as well as downtract smearing due to the spacecraft motion. The downtract IFOV varies between 350 and 840 m due to differences in the camera view angles. For MISR, observations are "oversampled" in that the distance the spacecraft moves between samples is less than the instrument IFOV. Thus, a given point location falls within the IFOV of multiple samples. The concept of a pixel is further complicated for MISR in that as many 4 × 4 (cross-track by along-track) pixels can be combined by the instrument and output as a single averaged pixel value. It is assumed that a "pixel" represents a signal as measured by a single detector element, unless explicitly stated. For the latter case "averaged pixel," or a descriptor such as "1 × 4 pixels" will be used.

Equal cross-track instantaneous fields of view (IFOVs) for the off-nadir cameras are provided by having four lens designs, named A–D, differing in focal length so as to compensate for variations in distance to earth. The cameras consist of a nadir camera (An) and two banks of cameras pointing in the forward (Af, Bf, Cf, and Df) and aftward directions (Aa, Ba, Ca, and Da) with respect to the spacecraft ground track. Images are acquired at the earth's surface with view angles of 0°, 26.1°, 45.6°, 60.0°, and 70.5°, fore and aft of zenith. The instantaneous view directions for the 36 data channels are depicted in Fig. 1. The actual camera boresight angles are 0°, ±23.3°, ±40.0°, ±51.2°, and ±58.0° (where the plus or minus sign indicates fore or aft viewing, respectively). These angles differ from the view angles at the surface due to the curvature of the earth. The instrument swath width provides global coverage every 9 days at the equator (2 days at the poles).

a. Camera design

Each camera uses four charge coupled device (CCD) line arrays per focal plane, 1504 photoactive pixels plus 16 light-shielded per array, with 21 μm × 18.5 μm pixels (cross-track by along-track). Each line array is filtered to provide one of four MISR spectral bands. The spectral profile is Gaussian in shape, which, used in conjunction with a Lyot depolarizer, will allow the instrument to be polarization insensitive.

1) LENS DESIGN

Each MISR camera consists of a lens barrel and a camera head that houses the focal plane structure and to which is attached the CCD driver electronics. The camera heads and electronics are identical for all nine cameras, leading to a modular design in which only the lens barrels are unique. The first-order properties of the four unique lens designs are shown in Table 1.
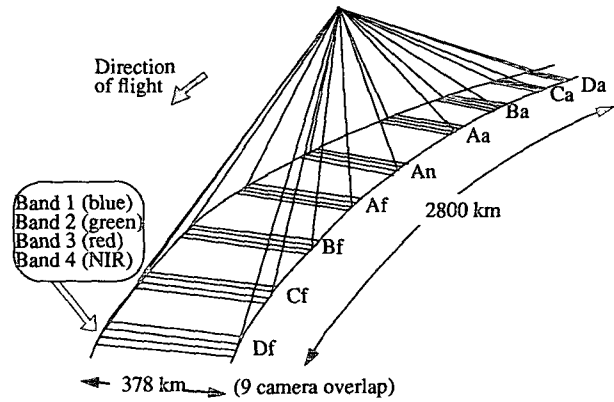

FIG. 1. MISR camera projections to earth.

Early in the lens design phase selected cerium-doped, radiation-resistent glasses were tested along with more conventional lens materials. After testing, at several times the anticipated EOS charged particle dose, it was demonstrated that transmittance losses at the MISR wavelengths were low (Al-Jumaily 1992). These data demonstrated that conventional lens glasses could be used, thereby extending the number of glasses available for the design. The final design is superachromatic (having a common focus at three MISR wavelengths) and thermally compensated for focus. It is a seven-element telecentric Biotar form. (In the telecentric design, the chief rays exit the cameras nearly parallel to the optical axis, independent of location in the field of view, with the benefit that the bandpass of the focal plane interference filters is nearly constant across the field.) An additional benefit of the telecentric design is that optical transmittance is only a weak function $(\cos^{-1}\theta)$ of field angle θ. To meet the system radiometric accuracy requirements, a double-plate Lyot depolarizer is incorporated into each of the cameras to scramble the polarization state. The effectiveness of Lyot depolarizers is dependent on the spectral bandwidth as well as the spectral band shape. They are most effective for Gaussian-like band shapes. Thus, the MISR filters are specified to have Gaussian band shape profiles to optimize the performance of the Lyot depolarizers.

Within the lens barrel, the lenses are mounted with a combination of aluminum and Rulon spacers with threaded aluminum retaining rings that clamp each lens–spacer assembly. The thickness of the Rulon has been calculated to match the lens–Rulon coefficient of thermal expansion to the expansion of the aluminum housing. Thus, the clamping force on the lens elements remains constant during thermal excursions. The centering of the lenses is controlled by the aluminum spacers that have been machined to be tangent to the lens element surfaces. Proper clearances prevent squeezing the lenses (which could result in breakage) during thermal cycling to the coldest survival temperature.

TABLE 1. MISR optics first-order parameters.

Camera design	Effective focal length (mm)	Field of view	View angle at earth's surface
A	59.3	±14.9°	0°, 26.1°
B	73.4	±12.1°	45.6°
C	95.3	±9.4°	60.0°
D	123.8	±7.3°	70.5°

Control of focus shift with temperature change is also provided using Rulon. The dominant factor affecting focus location for the cameras is the change of index of refraction of the glasses with temperature. Maintaining the position of the detector plane so that it coincides with the shifting focal plane of the lens requires moving the detector plane to follow the change in lens focus with temperature. The lenses were accurately modeled in CODE V and thermal excursions were simulated. The resulting thermal shift predictions were used to design a passive thermal compensation scheme. A cylinder of Rulon A was mounted between the detector housing, and a fiberglass tube used to thermally isolate the detector. The length of the Rulon was calculated to move the detector plane the needed distance and direction to maintain focus. For this focus concept to work, the Rulon needs to be nearly the same temperature as the lenses. This is accomplished through the thermal blanketing around the camera and through the high thermal conduction of the aluminum lens barrel and detector housing. Thermal gradients across the barrel are calculated to be less than 1°C.

2) FILTERS

The mosaic filter consists of four separate filter sticks epoxied into a single structure. When installed into the CCD package, each of the four CCD line arrays sees a different color. The filters are centered on 441, 555, 670, and 866 nm, which differ slightly from the system bandpass specification such that when the optics and CCD spectral responses are taken into account, the system requirements are met. The MISR filter specifications require a high degree of uniformity among all filters, as well as very stable and durable coatings that will not shift or degrade with age or environmental stresses. Ion-assisted deposition (IAD) technology has therefore been utilized. Manufacturing the passband and blocking layers on separate substrates prevents cost from being prohibitive. After the coating runs the two substrates are bonded together, with the coatings to the interior. Optical masks are incorporated into the assembly to prevent white-light leakage through the interfilter epoxy bonds. The completed filter is 650 μm (25.6 mil) thick.

3) DETECTORS

The MISR CCD architecture consists of four line arrays on a common piece of silicon, with a spacing of 160 μm (6.3 mil) center to center. The silicon die is mounted in a ceramic package. The filter defining the four optical bandpasses is aligned with the CCDs but is displaced above the focal plane by 38 μm (1.5 mil). The package has a laser-welded window, is back filled with argon, and hermetically sealed. The hermetic package prevents contamination of the filter and CCD elements, eliminates humidity, and improves stability. Integration time for each line array can be controlled independently. This allows for different integration times in different bandpasses in order to equalize radiometric performance and maximize signal-to-noise ratio. The arrays are operated at 50 kilopixels per second with a 40.8-ms line repeat time to provide 275 m of along-track separation between successive lines.

The MISR CCD's have a "thin poly" design, a new technology developed to increase the detectors' sensitivity to wavelengths shorter than 500 nm. The architecture is otherwise based on standard three-phase, three-poly, n-buried channel silicon detector technology. Additional processing is performed to create the thin-poly CCD. Specifically, the third poly deposition over the photogate (active pixel) region is etched down. This is followed by deposition of a thin fourth poly layer. This etching and deposition process is necessary to ensure that the poly layer thinning occurs over the photogate region only and to maintain continuous electrical contact throughout the entire line array. The thickness of the poly gate over the active pixels is about 40 nm, as compared to 200 nm for conventional devices.

The detector is cooled to -5°C with a single-stage Thermo-Electric Cooler (TEC). Temperature stability is within ±0.1°C, accomplished by computer control of a heater. The TEC is always on, and small amounts of heat are added to control the temperature. The heat generated by the TEC is conducted through the optical bench to which the nine cameras are attached and then radiated to space with a dedicated TEC radiator. Due to the mass of the optical bench, it remains thermally stable, with less than 2°C spatial or temporal gradients, throughout the orbit.

b. Instrument subsystems

1) STRUCTURE

The cameras are mounted to the optical bench at their front (light entrance) end with the detector end cantilevered into the instrument cavity. Light baffles are mounted to the optical bench in front of each camera. The detector assembly is mounted to the end of the lens barrel. Attached to the detector assembly is a small, low-powered electronics box that provides static charge protection to the detector, carries the tempera-

ture monitoring signals, and provides initial signal amplification. Thermal blanketing surrounds each camera to prevent thermal coupling between the cameras and the electronics inside the instrument cavity. The cameras are thermally tied to the optical bench. Each camera is designed to operate within the range of 0°–10°C.

The optical bench assembly is connected to the instrument structure with a system of titanium tubular bipods. To ease structural and thermal loads on the optical bench and supporting bipods, the design separates the camera support electronics from the camera head. The camera support electronics will be mounted on a thermally isolated structural platform. This platform will have thermal straps to conduct heat to a set of passive radiators. Each electronic box has a short cable that attaches to the respective camera head. The optical bench with attached optics will be thoroughly blanketed to protect it from internal heat radiation. The primary support structure enclosure walls are designed to maintain rigid support for the optical bench and provides kinematic attachment to the spacecraft. In addition, it provides a structural mount for the passive radiators located on the nadir-facing side of the instrument, houses the instrument system electronics and the flight computers, and incorporates optical baffles to keep specular glints from neighboring instruments from illuminating MISR's optical calibration surfaces.

2) ELECTRONICS

The MISR electronics fall into three general areas: camera electronics, system electronics, and calibration electronics. Each camera is relatively autonomous with its own power supply and serial data interfaces. The power supplies are 25-kHz sine wave supplies, which provide high efficiency with simultaneous low-noise performance. The camera electronics can stand alone through most testing and camera calibration. The design ensures that if an in-flight failure occurs in a camera's electronics it is not allowed to propagate to another camera or to the system electronics. The camera digital electronics provide interfaces to the system electronics controlling the camera as well as all the drive and timing signals to the CCD focal plane, the double-correlated signal chain, and the engineering signal conditioning (ESC) circuits. The signal chain amplifies and converts the CCD video into 14-bit digital numbers. There are four signal chains per focal plane for a total of 36 in the instrument. The signal chains are hybrids, providing both noise and mass advantages. All camera digital circuits reside on field-programmable gate arrays. This technology allows for increased packing densities and the speed of custom-application-specific integrated circuits with the programming ease of programmable read-only memories (PROMs).

The system digital electronics' main function is to interface the instrument to the platform. All system electronics are redundant to avoid the possibility of a single-point failure. The system electronics contains redundant 1750A computers with 1553-bus interfaces to the spacecraft. All commands from the spacecraft and engineering data go through the 1553 bus. The system electronics also provide the high-speed data interface, control inputs to the cameras, control power throughout the instrument, and control all of the mechanisms. A system ESC circuit measures system-wide temperatures and voltages. All nine TECs (one for each camera) are powered by the system power supply and placed in series. A diode is placed in parallel with each TEC such that a single TEC failure does not disable the entire string. As in the cameras, all of the custom digital circuits will reside on FPGAs.

It has been demonstrated that a true 13-bit digital representation of the measured radiance is sufficient to meet the radiometric needs identified by the science team (less would incur increased quantization noise). Square-root encoding, as well as the data averaging, is provided by the system electronics. These are implemented as a means of data compression, needed in order to meet the data rate constraints. Square-root encoding reduces quantization error at low signal levels at the expense of increased quantization error at high signal levels. This is an acceptable trade-off as photon noise is the dominant error source at the higher radiometric levels. During ground data processing the square-root encoding is reversed. This produces a DN dataset that is linear related to incident radiance. (At this time the DN are also padded to 16-bit filling, simply to package into machine words.)

The calibration electronics consists of the calibration diode preamplifiers and the ESC circuits associated with the diodes. The preamps are the transconductance type operating in the picoamp region. The calibration diodes have their own ESC circuits since all cameras may not be on during instrument calibration, due to power constraints.

c. Onboard calibrator

For both the preflight and in-flight calibrations MISR output are radiometrically calibrated using a spatially uniform source whose radiant output is determined using detector standards. Source standards rely on a series of radiometric comparisons from the National Institute of Standards and Technology (NIST), through a lamp vendor, and to the instrument flat-field calibration source. Conversely, detector standards are based upon manufacturing knowledge of photon to electron conversion efficiency, filter transmittance, and acceptance cone of illumination. It is believed that the MISR detector standards provide greater radiometric accuracy than would be obtained using source standards. During preflight testing, an integrating sphere and laboratory photodiode standards are utilized to achieve the radiometric calibration of the cameras. In-flight, MISR is calibrated using an onboard calibrator (OBC) that con-
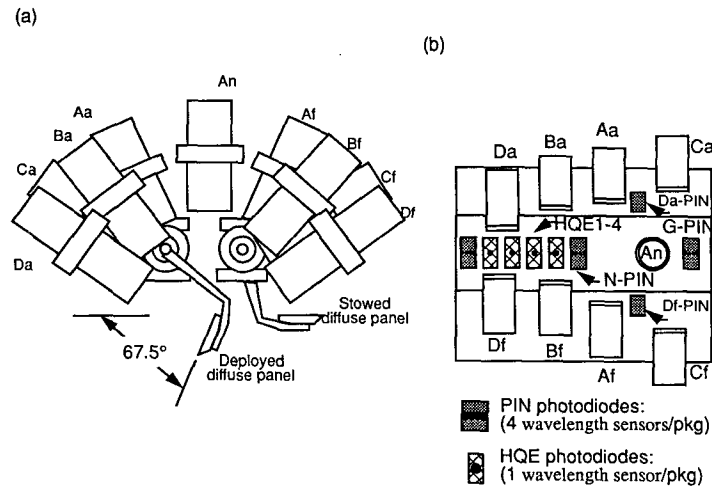
FIG. 2. Location of (a) the calibration panels and (b) photodiodes
on the optical bench.

sists of two Spectralon diffuse calibration panels, high quantum efficiency (HQE) diodes in a trapped configuration, and single (not trapped) radiation-resistant PIN diodes, including one mounted to a goniometer arm to provide angular characterization of the diffuse panels. Figure 2 shows the location of these elements with respect to the optical bench structure.

The panels are deployed for calibration at monthly intervals, except at mission start when multiple observations are collected the first month. Over the North Pole, one panel will swing aftward to reflect diffuse sunlight into the fields of view of the aftward-looking and nadir cameras. Over the South Pole, the other panel will swing forward for calibration of the forward-looking and nadir cameras. Thus, the nadir camera will provide a link between the two sets of observations. By monitoring the panels with photodiode assemblies, and through consistency checks using overflight campaign data, slow changes in panel reflectance are allowable without compromising the calibration accuracy, since the photodiodes provide the primary standard.

The time available for calibration will be about 7 min at each pole. In this time the cameras will see a range of illumination, through sunrise (sunset at the South Pole) onto the panel, to a view of the sun through a varying amount of earth atmosphere (including atmosphere-free space). By using the photodiodes to measure the panel-reflected radiances, the cameras can be calibrated using data covering the dynamic range of the sensor. In addition to these panel views, the cameras will gather data over the dark earth for 3 min each month. The dark-earth data will establish the dark current spatial variability across the array. Dark current is expected to be slowly varying during the mission, gradually increasing due to particle radiation exposure.

1) DIFFUSE PANELS

The panels are required to have a high, near-Lambertian reflectance. These properties are needed to direct sufficient energy into the cameras to reach the upper end of the sensor dynamic range. The Lambertian property also facilitates knowledge of the radiance into the cameras, as the radiance is measured by photodiodes at a particular panel view angle, and corrected for departure from Lambertian behavior. One challenging panel requirement is for uniformity in the reflected radiance field. This is necessary in order to accurately measure pixel-to-pixel and camera-to-camera differences in responsivity. To fulfill this requirement, scattering within the instrument is minimized, and baffles are provided to block the panels from a view of other instrument and spacecraft structures.

After a materials search, Spectralon has been selected as the material of choice for the MISR in-orbit calibration targets. Spectralon is a product of Labsphere (North Sutton, New Hampshire) and is composed of pure polytetrafluoroethylene (PTFE, or Teflon) polymer resin that is compressed into a hard porous white material using temperature and pressure sintering. No binders are used in the procedure. Spectralon is widely used in laboratory and ground/field operations as a reflectance standard. MISR has provided for the flight qualification of this material (Bruegge et al. 1993; Stiegman et al. 1993). Areas of investigation for flight qualification include static-charge build-up studies, optical characterization, environmental exposure (including UV, humidity, atomic oxygen and thermal cycling impact studies), measurement of mechanical properties such as tension and compression strengths, and vibration testing. The diffuse panels are stowed and protected while not in use. Cumulative space exposure time (deploy time) for

each panel is expected to be less than 100 h over the mission life. With these factors panel stability is expected to be high (changing less than 2% the first year and 0.5% per year thereafter).

Deployment of the panels, as well as the cover, will be actuated through the use of a mini-dual-drive actuator, providing redundancy and fault tolerance. A single motor is used for the goniometer. Redundancy is not implemented for the goniometer, since its failure would not be mission critical.

2) CALIBRATION PHOTODIODES

The diffuse calibration targets will be monitored by three types of diodes: radiation-resistant PIN photodiodes and two types of HQE diodes. (Note: "PIN" is a description of the diode architecture where p, intrinsic, and n doped layers are stacked.) The radiation-resistant photodiodes will be fabricated four to a package, each diode filtered to a different MISR spectral band. The fields of view are approximately 7°, sufficient to allow the required signal-to-noise ratio (SNR) of 500 to be achieved. Five such packages will be used. Two will view in the nadir direction, two in the Df and Da camera directions, and one package will be mechanized on a goniometric arm to monitor the angular reflectance properties of the panels.

The HQE's are in a "trap" configuration. Here three silicon photodiodes are arranged in a package so that light reflected from one diode is directed to another diode. The output of each diode is summed, resulting in near 100% quantum efficiency. A single spectral filter per package is used, and four such packages provide coverage at the four MISR wavelengths. One diode type will be used to obtain high quantum efficiency (QE) in the blue, and another type will be optimized for QE in the remaining three bands. The diodes have been specified to have an internal quantum efficiency exceeding 0.995, to have a front surface loss of less than 20%, to have a linearity of response better than 99.99% over an *equivalent reflectance* range of 0.05–1.0, and to have SNR in excess of 500 at full scale.

The equivalent reflectance parameter is used to specify instrument signal-to-noise requirements. This parameter is defined as

$$\rho_{eq} = \frac{\pi L_\lambda}{E_{0\lambda}}, \tag{1}$$

where L_λ is the spectral radiance incident at the sensor while observing a given target and $E_{0\lambda}$ is the spectral exoatmospheric solar irradiance at wavelength λ. (Both L_λ and $E_{0\lambda}$ are band weighted over the passband response.) To convert an equivalent reflectance into radiance, therefore, $L_\lambda = E_{0\lambda}\rho_{eq}/\pi$ where $E_{0\lambda}$ is the exoatmospheric solar spectral irradiance, as given by the World Climate Research Programme (Wehrli 1986).

3) GONIOMETER

The goniometer is a mechanized device that characterizes the relative diffuse panel radiance function with the angle. It does so in a plane parallel to the spacecraft flight direction. A PIN package mounted to the goniometer arm swings through ±60° to allow panel characterization appropriate to the along-track camera angles.

d. Data modes

1) GLOBAL MODE

There are several observational modes of the MISR instrument. Global mode refers to continuous operation with no limitation on swath length. Global coverage in a particular spectral band of one camera is provided by operating the corresponding signal chain continuously in a selected resolution mode. In addition to the mode in which data from a particular channel are not averaged, the instrument provides the capability, selectable for each channel by ground command, of averaging four cross-track by four along-track (4 × 4) pixels, 2 × 2 pixels, or 1 × 4 pixels. Without this capability the data rate would be prohibitively high. Any choice of averaging modes among the nine cameras that is consistent with the instrument data rate allocation (3.8 Mbit s^{-1} averaged over an orbit; 9.0 Mbit s^{-1} peak) is suitable for global mode. The nominal pixel averaging global mode envisioned for routine operations is given in Table 2.

2) LOCAL MODE

Local mode provides high-resolution images in all four bands of all nine cameras for selected earth targets. This is accomplished by inhibiting pixel averaging in all bands of each of the cameras in sequence, one at a time, beginning with the first camera to acquire the target (Df) and ending with the last camera to view the target (Da), a sequence that takes 7 min to complete. The instrument geometry limits the along-track length of local mode targets to about 300 km. This mode shall be used over the Mojave Desert, near Los Angeles, and White Sands, New Mexico, for instrument calibration

TABLE 2. Nominal global mode.

Camera	Spectral band			
	Blue	Green	Red	Near IR
Df, Da	1 × 4	4 × 4	1 × 1	4 × 4
Cf, Ca	1 × 4	4 × 4	1 × 1	4 × 4
Bf, Ba	4 × 4	4 × 4	1 × 1	4 × 4
Af, Aa	4 × 4	4 × 4	1 × 1	4 × 4
An	1 × 1	1 × 1	1 × 1	1 × 1

TABLE 3. Spectral specifications. Knowledge and stability specifications are equal for both center wavelength and bandwidth parameters.

Band	Center wavelength (nm)	Center wavelength uniformity (nm)	Knowledge (nm)	Stability (nm)	Bandwidth (nm)	Bandwidth uniformity (nm)
1	443	±1.0	±0.5	±1.0	25	±2.0
2	555	±1.0	±0.5	±1.0	15	±2.0
3	670	±1.5	±0.5	±1.0	15	±2.0
4	865	±2.0	±0.5	±1.0	25	±2.0

purposes, as well as up to about 100 other sites selected for various scientific objectives.

3) CALIBRATION MODE

In calibration mode the calibration photodiodes are activated, and data from the cameras and photodiodes are acquired. During calibration the cameras are ramped through a series of configurations that provide data through all integration times and data averaging modes, including the baseline global mode. Calibration mode will be used on a monthly basis during routine mission operations, although early in the mission it will be used more frequently.

4) ENGINEERING DATA

During flight the MISR instrument routinely transmits temperature measurements of the optical bench, optics, CCD, TEC, electronics, and photodiodes. These data are transmitted as part of the engineering data stream, both during routine science data acquisition and during in-flight calibration activities. These data are used in conjunction with the preflight characterization data to provide the appropriate calibration coefficients, where temperature dependence is a factor. Other engineering data include an unlatch flag for the cover and diffusers, deployed or stowed flags for the diffuse panels and cover, motor currents, power supply current, and photodiode radiometry.

3. Calibration requirements

In order to accomplish its scientific objectives, MISR is built to challenging performance specifications. Radiometric accuracy must be within ±3% (1σ) over high-reflectance, spatially uniform scenes, and polarization insensitivity is to be better than ±1%. The instrument must be unaffected by image blur and scattering to better than 2% for a 5% equivalent reflectance (e.g., ocean) scene 24 pixels distance from a high-contrast edge (e.g., a cloud boundary). All performance requirements must be met through the first 5 years in orbit. During the mission, data from the channels are sent to a ground processing center where they are radiometrically converted and coregistrated to within ±550 m along-track/±275 m cross-track (2σ).

a. Spectral and radiometric specifications

The instrument design specifications have been defined in several internal controlling documents, including the Instrument Science Requirements and the Instrument Functional and Design Requirements documents. Those specifications that drive the characterization plans for MISR are listed in this section. Spectral, radiometric, and stability specifications are given in Tables 3–6, respectively. All requirements are stated at the 1σ confidence level.

1) OUT-OF-BAND REJECTION

The system response is required to have an absolute transmittance in the rejection region of less than 0.1%, at any wavelength and to average no more than 0.01%, over any 100-nm interval. The rejection region is defined as all wavelengths shortward of $\lambda_{c,m} - 2\Delta\lambda_g$ plus all wavelengths longward of $\lambda_{c,m} + 2\Delta\lambda_g$ where $\lambda_{c,m}$ is the center wavelength (computed from a moments analysis), and $\Delta\lambda_g$ is the Gaussian full-width half-maximum (in-band best fit).

TABLE 4. Radiometric uncertainty specifications.

ρ_{eq} (%)	Maximum absolute uncertainty (%, 1σ)	Between elements	ρ_{eq} (%)	Maximum relative uncertainty (%, 1σ)
100	±3	Pixel to pixel	100	±0.5
5	±6	Pixel to pixel	5	±1.0
<5	Best possible	Band to band	100	±1.0
		Band to band	5	±2.0
		Camera to camera	100	±1.0
		Camera to camera	5	±2.0

TABLE 5. Temporal stability.

ρ_{eq} (%)	Maximum annual change in response (%)	ρ_{eq} (%)	Maximum monthly change in response (%)
100	2	100	0.5
5	4	20	1.0
		5	2.0

2) MODULATION TRANSFER FUNCTION

The cameras shall have a modulation transfer function equal to or greater than 20% at 23.8 cycles per millimeter at all field points within the specified field of view.

3) POLARIZATION

The peak-to-peak change in instrument response resulting from varying the plane of polarization, for a 100% linearly polarized stimulus, shall not exceed 2%.

4) CONTRASTING TARGET

Two related forms of contrasting target requirements exist. The first describes the response required of a cloud–ocean boundary-type scene (a ρ_{eq} = 100% half-plane adjacent to a ρ_{eq} = 5% half-plane). Here radiometry must be free of instrumental adjacency effects, to within 2%, at a 24-pixel distance from the boundary. The second target type describes the response required of a lake–surrounding land scene type (a ρ_{eq} = 5% target 24 × 24 pixels in size surrounded by a ρ_{eq} = 50% background). The center 8 × 8 pixels shall not be affected by the background, to within 2%.

b. Geometric specifications

1) GEOLOCATION AND REGISTRATION

Imagery from the nadir camera shall be geolocated with an uncertainty of ±250 m in both cross-track and along-track directions. Further, imagery of a particular land surface target from the nine cameras shall be spatially coregistered to the terrain with an uncertainty of ±275 m cross-track and ±550 m along-track (these are 2σ requirements). Because the 36 channels of image data are not intrinsically coregistered when acquired (see Fig. 1), this coregistration must be achieved in the ground data processing and is a prerequisite to the retrieval of geophysical parameters. MISR imagery shall also be projected to an ellipsoid situated at the surface. For these data, the registration uncertainty requirements are ±250 m cross-track and ±500 m along-track. The allowable land surface uncertainties are larger to enable attribution of a portion of the error budget to topographic relief errors.

2) POINTING

Boresight angles of the MISR cameras must be manufactured to tolerances within ±3.5 mrad (±12′) of nominal. In addition, pointing repeatability is to be achieved in flight to ±87 μrad (±18″), 3σ confidence, in pitch, roll, and yaw over the temperature range MISR will encounter in orbit. The tight repeatability requirement, relative to the looser manufacture tolerance, is to ensure that the image registration requirements are met with a minimum of ground data processing. Further, the MISR instrument stability shall be ±24 μrad (±5″) over 1 s, and ±39 μrad (±8″) over 420 s, 3σ confidence, in pitch, roll, and yaw.

4. Preflight testing

Some degree of testing of MISR flight hardware is done at the component, camera, and system levels, as well as after shipment and integration onto the spacecraft. The bulk of the performance data, however, are collected at the camera level of assembly. By characterizing each camera individually, testing can be spread sequentially over time and the test hardware is simplified. Camera testing is to be done using two MISR-dedicated thermal vacuum chambers. The camera-level approach to characterization also permits camera spares to be stored as calibrated, ready to fly hardware. The shorter system level tests are to be conducted in shared, more costly facilities. Radiometric stability is verified at the system level of assembly. Instrument geometric stability is characterized at the system level.

a. Component testing

1) CCD

Each detector is screened for linearity, full well, and dark current before assembly into an integrated focal plane package. Radiation testing, temperature and humidity cycling, and other aging studies are conducted on each wafer, from which actual CCD arrays are manufactured.

TABLE 6. MISR signal-to-noise ratio requirements.

No pixel averaging (all bands)		4 × 4 pixel averaging		
Equivalent reflectance	Minimum SNR	Band	Equivalent reflectance	Minimum SNR
100%	700	1	15%	250
70%	600		10%	225
50%	450	2	7%	300
20%	300		4%	200
2%	100	3	5%	325
<2%	Best possible		3%	200
		4	4%	300
			2%	200

2) FILTER

Filter specifications are verified on the flight coating plates, before assembly into the final mosaic form. Testing at this phase includes spectral response, spatial uniformity of response, and out-of-band rejection. Thermal and moisture cycling, and radiation testing is conducted on flightlike assembly pieces. Structural integrity is verified visually under a microscope.

3) LENS

Lens field of view, effective focal length, distortion and lateral chromatic aberration, modulation transfer function (MTF), relative aperture, and transmittance are verified before mating to a camera head.

b. Optical characterization

The first of the MISR thermal-vacuum chambers is called the optical characterization chamber (OCC). This chamber is used to test a lens for MTF, back-focal length, and distortion. It is also used to test a given camera (lens and camera head) for MTF, focus, IFOV, stray-light, and extended target response. Inside is an optical bench, loaded with a collimator, target wheel, and gimbal to which the camera is mounted. The gimbal is used to swing the camera such that it can view the source at any field position. The target wheel contains a number of pinhole sources for point-spread function mapping, as well as several extended targets. Illumination is provided by an external xenon source, with fiber optic feed. Testing proceeds in an automated fashion, with computer control of the gimbal. As the chamber has no windows, testing can be conducted independent of other clean-room activities. The "ground support equipment (GSE)" computer is used to acquire camera video and engineering data.

c. Spectral calibration

The second MISR thermal vacuum chamber is termed the radiometric characterization chamber (RCC). In this chamber the spectral, radiometric, and polarization studies are conducted. As the illumination sources for this chamber are external and transmitted through a large chamber window, provision must be made to isolate RCC tests from other clean-room activities. A 2.4 m × 4.9 m (8' × 16') tent, made of black plastic (Fraloc), envelopes the RCC test equipment and chamber window to provide the necessary light shielding.

The first test to be conducted on a given camera within the RCC is spectral calibration. Data collected by the calibration team will be used to determine

- equivalent square-band representation, including the central wavelength of each pixel (as well as the array average), including the out-of-band response;

- best-fit Gaussian representation, including the full-width at half-maximum (FWHM) response of each pixel and array average for the in-band region; and
- out-of-band suppression.

These data will describe the system and include the effects of the optics, filter, and detector response with wavelength.

For this test use will be made of a monochromatic source, recording the relative camera output as a function of wavelength. The camera under test will be placed within the RCC and view light emerging from the exit slit of a monochromator. The slit is wide enough to illuminate all four bands simultaneously. The monochromator will scan from 400 to 900 nm with a step size of 0.5 nm. The monochromator output spectral density is calibrated using unfiltered laboratory photodiode standards. A number of standards are used, which when combined monitor the source with a spectrally flat (or known) detector response.

Spectral calibration of the monochromator is also required periodically. Here the monochromator grating position versus output wavelength is determined. This is done by replacing the xenon lamp, used during the camera test, with a mercury vapor lamp. The latter source has known spectral lines. This calibration will be repeated as needed to ensure knowledge of the monochromator output to 0.25 nm.

d. Radiometric calibration

During radiometric calibration the relationship between an incident radiance field and camera digital output is established. This is done using an "ideal" target that emits or reflects unpolarized light, is uniform in space and angle, and lacks spectral features such as absorption lines. Through knowledge of this source exitance the calibration equation can be established for a sensor:

$$L_\lambda = G(\text{DN} - \text{DN}_0). \qquad (2)$$

Here, L_λ is the incoming spectral radiance at band center, DN is the sensor digital number output, G is the detector gain coefficient, and DN_0 is the offset digital number coefficient.

The accuracy with which this can be accomplished will determine the lower bound for uncertainty in radiance measured while viewing an earth scene. This uncertainty, however, will be applicable to a majority of scene types. The degradation in radiometric accuracy experienced while viewing a complex scene type is quantified through the camera polarization, contrasting-target response, stray-light rejection, and near-saturation characterizations.

During camera calibration, data are gathered through the sensor's dynamic range. For camera tests these data are used directly with the calibration equation. When the system electronics are included in the signal chain,

however, the camera 14-bit linearly encoded output data are square-root encoded to 12 bits through use of a look-up table stored in a PROM. The data must therefore be linearized by squaring before fitting to the calibration equation. During preflight calibration the majority of data will be taken without use of the system electronics. Consistency in calibration between the approaches will be verified.

During preflight testing, an ideal scene is simulated using an integrating sphere. With the sphere the following objectives can be accomplished:

- measurement of signal-to-noise ratios and through a range of incoming radiances;
- determination of the gain and offset coefficients for each pixel;
- estimation of calibration uncertainties at the 1σ confidence level;
- verification of shielded pixel measure of baseline subtraction (BLS) and dark current;
- verification of linear calibration equation or development of higher-order equation, as needed;
- determination of the calibration coefficient temperature dependence;
- characterization of camera response as a function of scene history (previous level of illumination); and
- comparison of measured system response to mathematical model.

Figure 3 depicts the test setup used during radiometric calibration. The aperture of the integrating sphere will overfill the field of view of each camera, independent of camera design. This simulates the earth-view geometry and allows inclusion of stray and scattered light sources. The sphere is 1.6 m (65") in diameter, has a 76 cm × 23 cm (30" × 9") exit port, and a 30-cm (12") external sphere with variable aperture. The sphere will be sequenced through a number of lamp-on settings, allowing digital data to be collected at 12 radiometric levels. At least three repetitions of data will be collected at any one radiometric setting. The coefficients in the calibration equation will be determined for each pixel using these data. A statistical approach called the "fidelity analysis" (Chrien et al. 1993) will be used to fit a straight line through the data and provide a measure of the uncertainty in this fit. The fidelity analysis approach is preferred to conventional least squares approach in that this uncertainty can be determined even at radiance levels not represented by the test. Other calibrations will be performed by varying the sphere from maximum to minimum and returning to a maximum radiance output setting, thus verifying calibration is independent of scene history. Radiometric calibrations will be performed at the CCD operating temperature, with system electronics placed in their minimum, nominal, and maximum operating temperatures (−10°, 10°, and 40°C), and at two different integration times.
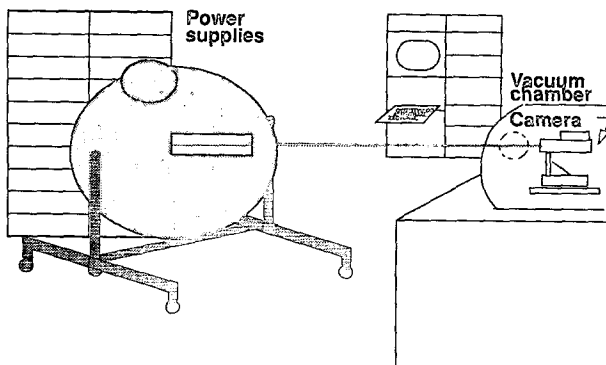

FIG. 3. Radiometric calibration setup.

The integrating sphere output will be calibrated using the laboratory diode standards and laboratory MISR filters. These components will be placed in the thermal vacuum chamber and view the sphere through the window. During this time the chamber will not be under vacuum, and the camera will not be present inside the chamber. Following this source characterization, the diode standards will be removed, the camera inserted into the chamber, and the chamber vacuum pumped for calibration. The integrating sphere incorporates a photodiode stability monitor that will provide a measure of sphere stability over the course of radiometric calibration. Radiometry is verified through round-robin intercomparisons with other EOS instrument teams, as well as with NIST. For the round-robins stable detector standards, provided by the National Research Laboratory of Metrology (NRLM) of Japan, and the Optical Sciences Center, Tucson, are used to view the various instrument sources in turn.

e. System tests

After camera characterization the cameras are mounted onto the MISR optical bench, along with the OBC elements. The optical bench is attached to the primary support structure along with the electronics and radiators to complete the instrument. At this level thermal, vibration, and camera pointing studies are conducted. Although radiometric calibration is not repeated at the instrument level, stability is verified.

1) RADIOMETRIC STABILITY

The test equipment used to verify radiometric stability is the MISR aliveness and stability test (MAST) tool. The MAST is a light fixture external to the MISR enclosure. It illuminates the deployed diffuse panels, thus providing a full-field illumination of each camera's FOV. It consists of a 1000-W xenon lamp, with a fiber-optic feed. The far end of the fiber bundle is attached to the instrument, clearing all glint baffle
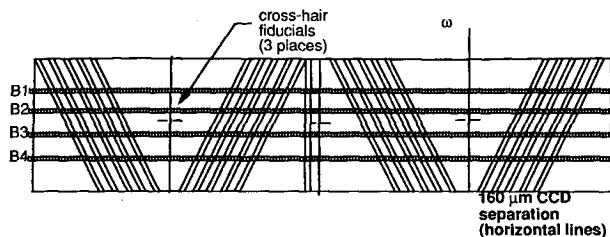
FIG. 4. CAT chevron test target used to establish relative camera pointing directions.

structures. There are two fiber bundles, one to illuminate each panel in turn. As the fiber has a vacuum feed, data can be acquired at ambient or vacuum pressures. Ambient-pressure, room-temperature data will be the baseline test condition. These tests will be conducted before and after instrument vacuum testing, post-ship of the instrument to the spacecraft integrator, and at the observatory level to verify that there is no instrument cross talk. (If possible, data will also be acquired at the Vandenberg launch hanger.)

2) POINTING

At the system level the pointing angles and their stability will be verified using the collimator array tool (CAT). This tool consists of a set of nine collimators that are precision mounted into a fixture at the nominal MISR camera boresight angles. This fixture is then mounted to the MISR instrument such that one CAT collimator corresponds to each MISR camera. MISR and the CAT will then be placed in a thermal vacuum chamber. Each collimator will then project the image of a precision-made chevron target into its corresponding MISR camera. This target is shown in Fig. 4. The image created on each MISR CCD will undergo centroid analysis to ascertain the boresight of the MISR cameras with respect to the CAT. Chevron CCD images will be collected as MISR is thermally cycled over the temperature range expected in orbit.

3) DIFFUSE PANEL UNIFORMITY OF ILLUMINATION

Verification of the uniformity of panel illumination will be done by using the integrating sphere as a uniform source. However, to achieve a more collimated output, the aperture will be cut to 2.5 cm × 51 cm (1″ × 20″) and the operating distance will be increased to 7.3 m (24′). This will produce rays that are "collimated" to within approximately 4° across the length of the calibration target. The increased operating distance reduces the sphere's output by about a factor of 36, but the IR channel will remain responsive since the sphere has a strong radiant output in the IR, as compared to a solar source. The nonuniformity measured with this configuration

will be compared to the nonuniformity measured during camera calibration. Any differences in uniformity will be due to back reflections and scattering of light onto the calibration targets.

5. In-flight characterization

MISR makes use of multiple sources of calibration data. The preflight test plans and OBC system were described previously. Other sources of calibration data include overflight calibration campaigns. These data will be combined to determine the uncertainty in sensor calibration.

a. Overflight calibration

After MISR is launched the radiometric calibrations established by the preflight and OBC analysis activities will be supplemented with an overflight calibration program. Here in situ surface bidirectional reflectance factor data are collected, and an atmospheric characterization is made over a region to be viewed by MISR in a high-resolution data mode (local mode viewing). With use of a radiative transfer code the radiance impinging on MISR is computed. This establishes an accurate calibration, particularly for the nadir camera.

b. Use of multiple calibration datasets

Use will be made of all datasets to provide the coefficients needed to describe the radiometric response of the instrument. It is required that data products be produced using timely data that reflect the current response function for the instrument. It is also required that there be no discontinuities in data products that are a result of abrupt changes in these calibration coefficients due to finite sampling and precision of the techniques. For this reason MISR will apply a smoothing function to the monthly calibration datasets. After the data are fit to a low-order polynomial curve, the calibration coefficients provided by the data fit are compiled. It is likely that this fit will be reestablished each month, using the last 10 (or so) measurement sets. Thus, after each new in-flight calibration activity using the OBC, a new set of coefficients will be computed. It is believed that each new coefficient set will vary only slightly from the previous. It is recalled that the instrument is being built to a stability specification of

TABLE 7. Level 1A product.

Product	Principal contents
Level 1A: Reformatted annotated product	• Data numbers linearized via square-root decoding • Navigation, engineering, and calibration data

TABLE 8. Level 1B1 radiometric product.

Parameter name	Horizontal sampling (coverage)	Comments
Radiance (W m^{-2} μm^{-1} sr^{-1})	250 m nadir, 275 m off-nadir, or averages per the camera configuration (global)	○ Radiometrically scaled data ○ No geometric resampling ○ 9 cameras, 4 bands ○ Uncertainty reported in ancillary radiometric product

0.5% limit on response change per month and 2% change limit per year.

Radiometric verifications to the calibration are enabled by comparing with the Moderate-Resolution Imaging Spectroradiometer (MODIS) and the Advanced Spaceborne Thermal Emission and Reflection Radiometer (ASTER) radiance products over common viewing locations, as well as using MODIS- and ASTER-derived radiance data from their respective field operations. MODIS and ASTER fly on the same spacecraft as MISR.

c. Science Computing Facility (SCF) image analysis

In-flight performance assessment of the MISR instrument will be conducted at the MISR Science Computer Facility. Here noise and dead pixel assessment will be conducted, trend analysis performed with the flight engineering data, relative calibration provided using scene studies, and the absolute radiometric coefficients determined from the multiple datasets. Radiometric uncertainty will be reported for both ideal targets (such as the calibration sites), and representative scene sites. The routine local mode data will be invaluable for these studies.

6. Data products

a. Reformatted annotated product

Square-root encoding is performed in flight in order to compress MISR data and prepare for transmission. Thus, the 14-bit data that are produced by an individual

camera are square-root encoded, through use of a table look-up process, and reduced to 12-bit numbers. At the lowest archive level for MISR data, level 1A, this step is reversed, then padded to a 16-bit word. That is, the level 1A data are representative of the original camera output in which the digital number (DN) values depend linearly on the input radiance. In addition to these camera DN values, the level 1A product is appended with platform navigation, MISR engineering parameters, and associated calibration coefficients, as shown in Table 7.

b. Radiometric product

The level 1A data are used as input to the level 1B processing code. The primary objective of the MISR level 1B1 processing algorithm is to produce MISR band-averaged radiances from the camera digital numbers (DN). The level 1B1 product also contains a clear-sky mask for each camera. These parameters are summarized in Table 8. The radiometric data are reported at the same spatial resolution as the input DN, and no resampling is performed. Processing is done routinely on all transmitted MISR data.

The algorithm used to produce the level 1B1 radiometric product requires knowledge of the radiometric calibration coefficients for each pixel. This instrument calibration is updated monthly with use of onboard calibrator (OBC) data and semiannually during field campaigns. The coefficients used in the radiometric product generation are documented in the ancillary radiometric product (ARP), summa-

TABLE 9. Level 1B1 ancillary radiometric product.

Parameter name	Comments
Data range	○ Revision number ○ Date/time range of applicability
Radiometric calibration coefficients (W m^{-2} μm^{-1} sr^{-1} DN^{-1}) (gain); DN (offset)	○ 1504 pixel values for both gain and offset for 9 cameras and 4 bands and at several temperatures
Camera calibration uncertainty (%)	○ 1504 pixel values for 9 cameras, 4 bands at 5 radiometric values
Dead pixel mask	○ Values 1 (responsive), 0 (dead pixel)
Spectral band parameters (center wavelength, bandwidth, transmittance) (nm)	○ Equivalent square-band and Gaussian representation provided
Instantaneous field of view (IFOV) (μrad)	○ Cross-track and along-track half-power points of pixel responsivity function with angle
Exoatmospheric spectral solar irradiances (W m^{-2} μm^{-1})	● Weighted over each MISR spectral band

TABLE 10. Level 1B2 products.

Product	Principal contents
Level 1B2: Georectified radiance product	• Resampled radiances projected onto space oblique Mercator grid • View and illumination geometric parameters
Ancillary geographic product	• Latitude and longitude of space oblique Mercator (SOM) grid points • Surface elevation and slope data • Surface classification data
Geometric calibration dataset	• Mapping transformations from image space to earth reference • MISR images acquired early in mission to which later data are registered • Parameters describing camera orientation, pixel view directions • Ground control points

rized in Table 9. Also included in the ARP is radiance uncertainty, spectral and instantaneous field-of-view information. The ARP is generated at the MISR SCF, updated as needed, and delivered to the DAAC (Distributed Active Archive Center). Thus, production of the ARP is not part of the routine DAAC processing of MISR data.

At a minimum radiance conversion will be implemented through a simple radiance scaling algorithm in which a gain and offset coefficient (specific to each pixel) are used in conjunction with a linear calibration equation. During preflight characterization the need to incorporate instrument correction terms will be determined. Contrast enhancement through point-spread function deconvolution, out-of-band response removal, and pixel nonuniformity corrections are to be considered. The need for these corrections is dependent on instrument performance, which is currently under evaluation.

c. Registered imagery

Following radiometric conversion, MISR images are geolocated and coregistered (angle to angle and band to band) to produce the level 1B2 georectified radiance product. Preparation for this processing begins at the SCF, where a set of reference orbits (233 orbits at nine view angles) are constructed from initially acquired, cloud-free, MISR scenes. These reference images are geolocated using ground control points. Subsequent MISR imagery are matched to the reference MISR datasets, with like view angles compared. Spacecraft-supplied navigation is used to provide a first guess at image geolocation for newly acquired data, and matching is performed as required. Thus the approach is adaptive to the platform attitude knowledge performance. The geometric camera model is obtained from the preflight testing program and refined once in orbit

using actual MISR imagery. The georectified radiance product, ancillary geographic product, and geometric calibration dataset contents are summarized in Table 10.

d. Science products

Level 2 products use these radiances to produce geophysical measurements of aerosols, surface bidirectional reflectance factors, and cloud parameters. The at-launch standard data products that are to be routinely generated at the National Aeronautics and Space Administration Langley DAAC are summarized in Table 11. More information on these products is available within the MISR project documents, such as the MISR data product description (DPD) document. These are listed in the reference section, and are soon to be made available on the World Wide Web (http://www-misr.jpl.nasa.gov). In addition to the routinely generated standard products, there are a number of ancillary data products and datasets that are generated at the MISR SCF and archived at the DAAC. These aid in the production or interpretation of the standard data products.

7. Summary

MISR has recently completed a critical design review. Much of the test equipment needed to characterize both the engineering model and flight units has been procured. Testing of the engineering model will confirm the approaches described here and allow the team to gain experience with handling the large volumes of data to be produced by the MISR instrument. After

TABLE 11. Level 2 products.

Product	Principal contents
Level 2: Top of atmosphere (TOA)/cloud product	• Top-of-atmosphere (TOA) bidirectional reflectance factor (BRF) • TOA albedo at reflecting-level reference altitude (RLRA) and at a 30-km reference altitude • Reflecting-level classifiers, including elevation • Cloud fraction (low, medium, and high clouds)
Level 2: Aerosol/surface product	• Tropospheric aerosol optical depths and compositional model identifiers • Surface hemispherical-directional reflectance factor (HDRF) • Surface bihemispherical reflectance (BHR) • Ancillary meterological and atmospheric data

been refined, the team will begin characterization and calibration of the flight hardware.

Acknowledgments. The design, fabrication, and characterization of the MISR instrument is credited to a large number of individuals. The design and characterization plans described in this text are attributed to the efforts of Hershal L. Fitzhugh and S. Teré Smith (camera testing and system integration and test), Ghobi Saghri (spectral and radiometric testing), Carlos Jorquera (photodiode standard and flight diodes), Nadine Chrien (system analyst), Robert P. Korechoff (optical performance assessment), Eric B. Hochberg (optical testing), Brendan McGuckin and David Haner (Spectralon testing), Bidushi Bhattacharya (data and software archive), Neil Pignatano (Ground Support Equipment), Mary White (lens fabrication and test), Enrique Villegas (CCD fabrication and test), Virginia Ford (camera and diode optomechanical design and fabrication), Jewel Beckert and Elmer Floyd (instrument managers), Don Rockey and Gary Francis (system engineers), and Terrence H. Reilly (project manager). The work described in this paper is being carried out by the Jet Propulsion Laboratory, California Institute of Technology, under contract with the National Aeronautics and Space Administration.

REFERENCES

Bruegge, C. J., A. E. Stiegman, R. A. Rainen, and A. W. Springsteen, 1993: Use of Spectralon as a diffuse reflectance standard for inflight calibration of earth-orbiting sensors. *Opt. Eng.* 32(4), 805–814.

Chrien, N. C. L., C. J. Bruegge, and B. R. Barkstrom, 1993: Estimation of calibration uncertainties for the Multi-angle Imaging SpectroRadiometer (MISR) via fidelity intervals. *Proc. SPIE.* 1939, 114–125.

Al-Jumaily, G. A., 1992: Effects of radiation on the optical properties of glass materials. *Proc. SPIE,* 1761, 26–34.

MISR data product description, JPL D-11103, Rev. A, December 1994.

MISR instrument science requirements, JPL D-9090, Rev. A, August 1994.

MISR instrument functional and design requirements, JPL D-9988, Rev. A, November 1994.

MISR level 1B1 algorithm theoretical basis: Radiometric product, JPL D-11507, Rev. A, November 1994.

MISR level 1B2 algorithm theoretical basis: Geo-rectified radiance product, JPL D-11532, Rev. A, December 1994.

MISR level 2 algorithm theoretical basis: Aerosol/surface product, Part 1 (aerosol parameters). Product, JPL D-11401, Rev. A, December 1994.

MISR level 2 algorithm theoretical basis: Aerosol/surface product, Part 2 (surface parameters) Product, JPL D-11401, Rev. A, December 1994.

MISR level 2 algorithm theoretical basis: TOA/cloud product, JPL D-11507, Rev. A, December 1994.

Stiegman, A. E., C. J. Bruegge, and A. W. Springsteen, 1993: Ultraviolet stability and contamination analysis of Spectralon diffuse reflectance material. *Opt. Eng.,* 32(4), 799–804.

Wehrli, C., 1985: Extraterrestrial solar spectrum. World Radiation Center, WRC Publ. 615, Davos-Dorf, Switzerland, July.